International Journal for Housing Science and Its Applications
Publish August 6, 2025. Volume 46, Issue 3 Pages 6350-6360

https://doi.org/10.70517/ijhsa463545

Effect of asphalt pretreatment on the pore structure and electrochemical behavior of porous charcoal studied by numerical simulation methods

Haocheng Xiong[1,*] and Haowen Zheng[1]
[1] School of Civil and Resources Engineering, University of Science and Technology, Beijing, 100083, China
Corresponding authors: (e-mail: 13071130135@163.com).

Abstract Bitumen is often used as a precursor for the preparation of carbon materials due to its high carbon content and abundant resources. Bitumen-based carbon materials have a high degree of graphitization, fewer defects and higher electrical conductivity, which have potential applications in energy storage. In this study, the effect of asphalt pretreatment on the pore structure and electrochemical behavior of porous carbon was investigated. Numerical simulation methods were used to prepare nine porous carbon materials from coal liquefied bitumen, medium-temperature bitumen and high-temperature bitumen by preoxidation, catalytic polymerization and high-temperature polymerization pretreatments, and analyze their structural characteristics by elemental analysis, XRD and Raman spectroscopy, determine the pore structural parameters by nitrogen adsorption-desorption isotherms, and use constant current charging/discharging, cyclic voltammetry and AC impedance spectroscopy to The electrochemical properties were evaluated by constant current charging and discharging and AC impedance spectroscopy. The results show that the heat treatment temperature directly affects the microcrystalline structure and pore size distribution of the porous carbon, and the carbon layer spacing d002 reaches a maximum value of 0.427 nm during the heat treatment at 430 ℃, indicating that it is the most disordered. The sample of PCs-370 possesses a maximum specific surface area of 2160 m²/g, with a microporous volume percentage of 91%. In terms of electrochemical performance, PCs-460 showed the best performance in the three-electrode system, with a specific capacitance of up to 422F/g at 0.5A/g current density, and remained above 290F/g at 10A/g current density. The results proved that porous carbon materials with excellent electrochemical properties can be prepared after appropriate pretreatment and activation of bitumen, which is of great significance for the design and preparation of electrode materials for high-performance supercapacitors.

Index Terms bitumen pretreatment, porous carbon, pore structure, electrochemical performance, supercapacitor, numerical simulation

I. Introduction

Bitumen, a heavy organic by-product from coal or petroleum processing, is a mixture of mainly small-sized, low condensed aromatic molecules, which is usually used as a precursor for the preparation of carbon materials due to its high carbon content and abundant resources, and has become a potential material in the field of energy storage due to its relatively high degree of graphitization, fewer defects, and higher electrical conductivity [1]-[4]. There have been many studies on bitumen-based carbon materials as supercapacitor electrode materials, and alkali activation, template carbonization, and heteroatom doping are commonly used to enhance the electrochemical properties of bitumen-based carbon materials [5]-[7]. However, when asphalt is used as a porous carbon precursor, the characteristics such as wide molecular weight distribution and complex composition lead to the need for different degrees of pretreatment for the target product requirements during its preparation [8]-[10]. Therefore, the effect of asphalt pretreatment on the pore structure and electrochemical behavior of porous carbon was investigated with a view to providing guidance for the preparation of asphalt-based porous carbon.

Generally speaking, asphalt is pre-oxidized to increase oxygen-containing functional groups, and cross-linking and condensation between these groups can regulate the morphology and properties of asphalt-based carbon materials [11]-[13]. The catalytic polymerization of asphalt can play a similar role to the pre-oxidation treatment, and the high-temperature polymerization of asphalt can form structures with different optical properties, which play different roles in the preparation of porous carbon, and the high-temperature polymerization is also conducive to the improvement of the yield of porous carbon [14]-[17].

Bitumen, a heavy organic by-product of coal or petroleum processing, is a mixture of mainly small-sized aromatic molecules with low degree of condensation, which is usually used as a precursor for the preparation of carbon

materials due to its high carbon content and abundant resources, and has become a potential material in the field of energy storage due to its relatively high degree of graphitization, fewer defects, and higher electrical conductivity. There have been many studies on bitumen-based carbon materials as supercapacitor electrode materials, and alkali activation, template carbonization, and heteroatom doping are commonly used to enhance the electrochemical properties of bitumen-based carbon materials. However, when asphalt is used as a precursor of porous carbon, the characteristics of wide molecular weight distribution and complex composition lead to the need for different degrees of pretreatment for the target product requirements during the preparation process. Therefore, the effect of asphalt pretreatment on the pore structure and electrochemical behavior of porous carbon was investigated with a view to providing guidance for the preparation of asphalt-based porous carbon.

Generally speaking, asphalt is pre-oxidized to increase oxygen-containing functional groups, and cross-linking and condensation between these groups can regulate the morphology and properties of asphalt-based carbon materials. The catalytic polymerization of asphalt can play a similar role as the pre-oxidation treatment, and the high-temperature polymerization of asphalt can form structures with different optical properties, which play different roles in the preparation of porous charcoal, and the high-temperature polymerization is also conducive to the improvement of the yield of porous charcoal. From the existing studies, there is a close correlation between the pore structure characteristics of porous carbon materials and their electrochemical properties. Micropores provide a large number of active sites for charge storage, while mesopores contribute to the rapid transport of electrolyte ions, which in turn improves the charging and discharging rates. By rationally designing the asphalt pretreatment scheme, the pore size distribution can be optimized while maintaining a high specific surface area, thus enhancing the comprehensive performance of porous carbon materials in supercapacitors. In recent years, numerical simulation methods have been increasingly used in material design and optimization, and the quantitative relationship between pretreatment parameters and material properties can be analyzed in depth through the establishment of a porous carbon structure model to provide theoretical guidance for experiments.

In this study, the mechanism of the influence of different pretreatment conditions on the structure and electrochemical properties of asphalt-based porous carbon was systematically investigated by using numerical simulation combined with experimental validation. By designing different KOH/asphalt ratios, activation temperatures, and asphalt pretreatment temperatures, a variety of porous carbon materials were prepared and fully characterized. Focusing on the chemical reactions occurring during the pretreatment process and their effects on the microstructures of the final products, the correlation model between the pretreatment parameters and the pore structure characteristics as well as the electrochemical performances of the porous chars was established. In addition, this study also investigated the effects of different types of asphalt feedstocks on the properties of the final products to provide a basis for selecting suitable asphalt precursors. Through the comparative analysis of the performance of different samples in supercapacitors, the intrinsic mechanism of asphalt pretreatment to optimize the performance of porous carbon electrode materials was revealed, which provides new ideas for the design and preparation of high-performance porous carbon materials.

II. Experimental design

II. A.Raw materials and experimental reagents

Coal liquefied residue (CLR) and coal liquefied pitch (LP) used in the experimental study were obtained from SH Coal Oil Chemical Co. and medium temperature pitch (MP) and high temperature pitch (HP) were purchased from WX Chemical Technology Co. The industrial and elemental analyses of the coal liquefied oil residue are shown in Table 1.

Table 1: Proximate and ultimate analyses of coal liquefaction residue

Industrial analysis (%)			Elemental analysis (%)			
Mad	Ad	Vdaf	Cdaf	Hdaf	Ndaf	St, d
0.76	15.82	37.25	91.28	5.06	1.06	1.89

The results of industrial and elemental analyses of the three bitumens are shown in Table 2.

Table 2: Proximate and ultimate analyses of pitches

	Industrial analysis (%)			Elemental analysis (%)				
	M	A	V	C	H	N	S	O*
LP	0.14	0.14	45.40	90.93	5.34	1.12	0.30	2.36
MP	0.21	0.19	61.28	91.25	4.96	1.16	0.64	2.04
HP	0.23	0.32	57.12	92.46	4.57	0.93	0.50	1.94

II. B.Experimental apparatus

The names, models and manufacturers of the instruments used in the experiment are shown in Table 3.

Table 3: Chemical reagents used in experiments

Chemical formula	Specification	Producer
KOH	Analytical purity	Shanghai Aladdin biochemical technology co., LTD
C4H6O4Mg·4H2O	Analytical purity	National drug collectivization co., LTD
HCl	Analytical purity	National drug collectivization co., LTD
HNO3	Analytical purity	National drug collectivization co., LTD
C6H12	Analytical purity	Tianjin coriochemical reagent co., LTD
C6H14	Analytical purity	Tianjin coriochemical reagent co., LTD
C6H6	Analytical purity	Tianjin coriochemical reagent co., LTD
C7H8	Analytical purity	National drug collectivization co., LTD
C8H10	Analytical purity	Tianjin coriochemical reagent co., LTD
C4H8O	Analytical purity	National drug collectivization co., LTD
……		

II. C.Porous Carbon Preparation

(1) Preparation of CKx-y series samples

A certain amount of KOH and 5 g of coal liquefied asphalt were mixed and ground (according to the mass ratio of 1:1, 2:1, 3:1), and the temperature was increased to the specified temperatures (700, 900 °C) in a nitrogen atmosphere of 200 mL/min at an elevated temperature rate of 10 °C/min, and the temperature was maintained at a constant temperature for 2 h. The samples were cooled down naturally to room temperature, and then washed with hydrochloric acid and deionized water to be neutral, and then dried at 150 °C for 12 h. The prepared samples were labeled as CKx-y, where x was the mass ratio of KOH and coal liquefied asphalt, respectively, 1:1, 2:1 and 3:1. The prepared samples were labeled as CKx-y, where x is the mass ratio of KOH and coal liquefied bitumen, 1:1, 2:1, 3:1, respectively, and y is the roasting temperature, 700, 900 °C, respectively. e.g., CK2-700 denotes the porous carbon prepared with the mass ratio of KOH and coal liquefied bitumen of 2:1, and the activation temperature of 700 °C. The prepared samples were labeled as CK2-700, where x is the mass ratio of KOH and coal liquefied bitumen, 2:1, 3:1, respectively, and y is the roasting temperature, 700, 900 °C, respectively. The prepared samples are labeled CK2-700 and CK2-900, respectively.

(2) Preparation of PCs-x series samples

4 g of coal liquefied bitumen, 12 g of Mg(CH3COO)2 and 9.50 g of KOH were mixed and milled, and the mixture was evenly spread in a corundum boat, and then ramped up to 800 °C at an elevated temperature rate of 5 °C/ min in a tube furnace, with a constant temperature in an N2 atmosphere for 2 h. The product was washed with a mixture of 1 mol/L HCl + 1 mol/L HNO3 and distilled water to remove impurities. The prepared sample was named PCs-9 after drying at 110 ℃ for 12 h. Other preparation conditions remained unchanged, the prepared samples were named PCs-0, PCs-6 and PCs-12 when the mass of KOH was 0 g, 6.34 g and 12.72 g, respectively.

(3) Preparation of PCs-y series samples

A certain amount of coal liquefied asphalt was loaded into a high temperature autoclave, purged with nitrogen and closed, and the temperature was increased to 400 °C at a rate of 3 °C/min, and then to the target temperatures (380, 420, 450, 480 °C) at a rate of 1 °C/min for 4 h. After the end of the thermostatic period, the pressure was released from the autoclave, and the lightweight component was purged with nitrogen, then the product was removed and labeled as PCs-0, PCs-6, and PCs-12, respectively. After cooling to room temperature, the products were removed and labeled as LP-370, LP-400, LP-430 and LP-460, respectively. 3 g of the polymerization products at different temperatures were mixed with 9.47 g of KOH and ground, and then the temperature was increased to 800 °C at a rate of 5 °C/min in a nitrogen atmosphere of 300 mL/min, and then the temperature was maintained at a constant temperature for 2 h. The samples were cooled down naturally to room temperature, and then washed to

neutral with hydrochloric acid and deionized water, respectively. The samples were washed to neutral with hydrochloric acid and deionized water, respectively, and dried at 110 °C for 12 h. The prepared samples were labeled as PCs-370, PCs-400, PCs-430, and PCs-460, respectively.

II. D.Electrode preparation and its electrochemical performance testing

The electrode sheet was prepared as follows, according to the mass ratio of carbon material: acetylene carbon black: polytetrafluoroethylene = 8:1:1, and add a certain amount of ethanol to fully grind, uniformly coated on the pre-treated nickel foam, the mass of the active substance per unit area was 2-4 mg/cm², and electrode sheets were made under the pressure of 8 Mpa and then vacuum dried at 80°C for 12 h. The electrode sheet was dried at 80°C for 12 h with a KOH solution of 6 molL as the electrolyte, Pt electrode as counter electrode and Hg/HgO electrode as reference electrode, constant current charge/discharge (GCD), cyclic voltammetry (CV) and ac impedance spectroscopy (EIS) tests were carried out in an electrochemical workstation (VersaSTAT4). Two electrode sheets with the same active material loading were tested in a two-electrode system and the cycling performance of the materials was tested.

In the three-electrode system, the specific capacitance of the supercapacitor can be calculated from the GCD curve by Eq. (1) or from the CV curve by Eq. (2):

$$C_s = \frac{I\Delta t}{m\Delta V} \tag{1}$$

$$C_g = \frac{\int_{V_1}^{V_2} i(V)dV}{ms\Delta V} \tag{2}$$

where C is the specific capacitance (F/g), I is the discharge current (A), Δt is the discharge time (s), m is the mass of the active substance (g), ΔV is the voltage window (V), $i(V)$ is the current (A), s is the scanning rate (5, 10, 20, 50, 100~mV/s) and V_1, V_2 are the lower and upper limits of the voltage window (V).

In the two-electrode system, two electrode sheets with the same porous carbon loading prepared by the above method were tested in 6 mol/L KOH electrolyte. The specific capacitance (C, F/g) of the single electrode was calculated according to Eq. (3), and the energy density (E, Wh/kg) and power density (P, W/kg) were calculated according to Eqs. (4) and (5), respectively:

$$C = \frac{4\times I\Delta t}{m\Delta V} \tag{3}$$

$$E = \frac{C\Delta V^2}{2\times 3.6} \tag{4}$$

$$P = \frac{3600E}{\Delta t} \tag{5}$$

where C is the specific capacitance (F/g), I is the discharge current (A), Δt is the discharge time (s), m is the total mass of active substance (g), and ΔV is the voltage window (V).

II. D. 1) Working Electrode Preparation

The preparation process of the working electrode is shown in Figure 1, the porous carbon material, conductive carbon black (C65, conductive agent), and polytetrafluoroethylene (PTFE, binder) are evenly mixed and ground in the ratio of 85:10:5 until they become flakes, and then the flake mixture is placed in a mold, and the mixture is pressed into a circular sheet with a diameter of about 13 mm with a pressure of 6 MPa, and finally the disc is made on the current collector foam nickel to make the working electrode [18].

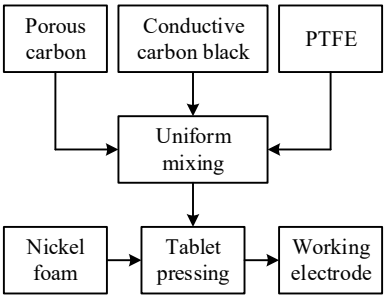

Figure 1: The preparation process of the working electrode

II. D. 2) Constant current charge/discharge test

Constant current charge/discharge test:

$$C_g = \frac{I\Delta t}{m\Delta V} \tag{6}$$

Constant current charge/discharge (GCD) is one of the important methods to study the electrochemical performance of porous carbon as a supercapacitor electrode material. In general, an ideal GCD curve is a standard "isosceles triangle", but in practice, a voltage drop occurs during discharge due to the presence of capacitor internal resistance [19].

In the three-electrode system, the calculation of the specific capacitance (Cg, Fg-1) can be obtained according to the following equation:

Where I(mA) is the discharge current during constant current charging and discharging, Δt(s) is the discharge time, m(g) is the mass of the active material on the working electrode, and $\Delta V(mV)$ is the voltage difference after removing the voltage drop during the discharge process.

In the two-electrode system, the calculation of the specific capacitance (C_s , Fg-1) can be obtained according to the following equation:

$$C_s = \frac{4I\Delta t}{m\Delta V} \tag{7}$$

where m(g) is the sum of the mass of active material on the two working electrodes, and other parameters are the same as in Eq. (8).

The energy density (E, Whkg-1) and power density (P, Wkg-1) of the supercapacitor were calculated according to Eqs. (8) and (9):

$$E = \frac{C_s \Delta V^2}{2 \times 4 \times 3.6} \tag{8}$$

$$P = \frac{3600E}{\Delta t} \tag{9}$$

II. D. 3) Cyclic Voltammetry

Cyclic voltammetric curves (CV) are curves in which a voltage signal that changes linearly at a constant rate is applied to the working electrode and the reference electrode, and the response current at the working electrode is recorded as a function of voltage. Scanning is carried out with different scanning rates, and the current response versus voltage is recorded by an electrochemical workstation. From the recorded current-voltage relationship curve, the microscopic reaction process on the surface of the working electrode and the reversibility of the electrode reaction can be determined. Theoretically the ideal shape of the porous carbon CV curve is a standard rectangle, but in practice, by the presence of dry pseudocapacitance and polarization, the resulting CV curve is not a standard rectangle, but a rectangle-like shape. The CV curves of the porous carbon electrodes in this thesis at different scan rates were obtained by testing at a Vertex. 1A. type EIS electrochemical workstation [20].

II. D. 4) Electrochemical impedance testing

Electrochemical impedance spectroscopy (EIS), also known as AC positive impedance spectroscopy, is an important method for studying capacitor resistance properties and electrode process kinetics. In this thesis, the AC impedance of a supercapacitor is tested by a Vertex. 1A. EIS type electrochemical workstation in the frequency range of 10-3 to 106 Hz with an applied AC signal amplitude of 10 mV [21].

II. D. 5) Cyclic Stability Testing

Cycling stability is an important index to evaluate the performance of supercapacitors. Cycling performance refers to charging and discharging the capacitor several times repeatedly at a fixed current, and analyzing the change of its performance such as specific capacitance and coulombic efficiency with the increase of the number of cycles [22]. In this thesis, a CT-4008-5V50mA-164 battery tester was used to test the cycling performance of supercapacitors. In this case, the capacitance retention (R, %) and Coulombic efficiency (η , %) of the capacitor were calculated according to Eqs. (10) and (11), respectively:

$$R = \frac{C_n}{C_1} \times 100\% \tag{10}$$

$$\eta = \frac{T_d}{T_c} \times 100\% \tag{11}$$

where C_n (Fg-1) is the specific capacitance after the nth cycle, C_1 (Fg-1) is the specific capacitance of the 1st cycle, and T_d and $T_c(s)$ are the discharge time and charging time of the nth cycle, respectively.

III. Results and discussion

In this paper, the porous carbon of CKx-y series, PCs-x series and PCs-y series, totaling nine raw materials, were used as precursors, and KOH and hydrochloric acid solutions were used as reagents for the experiments in this paper.

III. A. Pore Structure Analysis of Porous Carbon

In order to understand the changes of elemental composition of CK2, PCs after heat treatment, elemental analysis was carried out, and the results are shown in Table 4, with the increase of heat treatment temperature, the content of C and N elements gradually decreased, and the content of O and H elements gradually increased. Among them, the larger changes were in C and O elements, the mass ratio of C elements changed from 97.94% to 89.27%, a decrease of 8.67%, while the mass ratio of O elements changed from 1.22% to 9.07%, an increase of about 8%, which indicates that the heat treatment temperature has an effect on the secondary cross-linking as well as the subsequent pyrolysis, and that the secondary cross-linking reaction is relatively thorough and the oxygen content is relatively low during the heat treatment at 400°C. The results are shown in Table 4. The uncrosslinked sample CK2-700 has relatively high C element content and low oxygen content.

Table 4: Elemental analysis of different samples

Samples	C (wt.%)	N (wt.%)	H (wt.%)	O* (wt.%)
CK2-700	97.94	1.08	0.96	1.22
CK2-900	94.42	0.96	1.85	3.69
PCs-0	92.05	0.90	1.84	5.38
PCs-6	91.36	0.91	1.95	6.02
PCs-12	89.27	0.85	2.07	9.07

The data shows the effect of pre-treatment heat treatment on the microcrystalline size or the degree of disorder of the activated porous carbon material, with the change of heat treatment temperature, the carbon layer spacing d002 and AD/AG show a minimum value at the pre-treatment temperature of 370°C, indicating better ordering. From the XRD and Raman analysis data summarized as shown in Table 5, it can be seen that the heat treatment temperature affects the microcrystalline size as well as the degree of disorder of the material. With the increase of heat treatment temperature, the maximum value of carbon layer spacing d002 occurs at a heat treatment temperature of 430°C, indicating the largest degree of disorder. The trend of D-band and G-band integral area ratio AD/AG is consistent with that of d002. This is due to the different degrees of secondary cross-linking, pyrolysis and polycondensation reactions occurring at different temperatures, resulting in structural differences. The secondary cross-linking reaction is more sufficient when the heat treatment temperature is 600 ℃, which inhibits the generation of ordered structures to a certain extent, forming a more disordered structure.

Table 5: Physical parameters of different samples

Samples	d002 (nm)	Lc (nm)	La (nm)	AD/AG
CK2-700	0.412	0.236	0.456	3.08
CK2-900	0.411	0.232	0.457	3.24
PCs-0	0.396	0.232	0.449	3.06
PCs-6	0.394	0.233	0.451	3.09
PCs-12	0.420	0.228	0.442	3.02
PCs-370	0.415	0.227	0.440	2.96
PCs-400	0.418	0.224	0.446	2.98
PCs-430	0.427	0.229	0.447	3.00

The pore structure parameters of the material are shown in Table 6, the microporous volume with the heat treatment temperature shows a trend of increasing and then gradually decreasing, the mesopore volume shows a gradual increase in the trend of the heat treatment temperature of 370 ℃ porous carbon specific surface area is the largest, amounting to 2160m ² / g, the microporous volume of the proportion of 91%. When the heat treatment temperature is 6℃, the specific surface area can reach 745m²/g. It can be seen that the crosslinking treatment is

given to the sample surface functional groups by a certain temperature heat treatment pyrolysis, the formation of the bulk phase structure contains rich pores. From the pore size distribution, it can be seen that the pore size of the heat-treated sample is mainly concentrated below 1 nm.

Table 6: Pore-structure parameters of samples

Samples	SBET (m²/g)	Vtot (cm3/g)	Vmicro (cm3/g)	Vmeso (cm3/g)	Vmicro /Vtot (%)	Vmeso /Vtot (%)
CK2-700	542	0.36	0.24	0.15	0.64	0.39
CK2-900	598	0.38	0.24	0.14	0.68	0.34
PCs-0	634	0.3	0.24	0.17	0.63	0.40
PCs-6	745	0.42	0.30	0.14	0.70	0.33
PCs-12	1356	0.75	0.70	0.04	0.98	0.06
PCs-370	2160	1.04	0.91	0.14	0.89	0.14
PCs-400	1723	0.85	0.74	0.16	0.84	0.20
PCs-430	1528	0.86	0.63	0.28	0.75	0.30
PCs-460	210	0.22	005	0.18	0.20	0.87

III. B. Electrochemical performance analysis

(1) Constant current charge/discharge (GCD)

The constant-current charge-discharge curves of the nine porous charcoals at 0.5 A/g current density are shown in Fig. 2. In the voltage window of -1V~0V, the constant-current charge-discharge curves of the nine coal pitch-based porous carbon materials all show symmetric triangular characteristics, which is a unique charge-discharge curve characteristic of the double layer capacitor. Fig. 2(b) shows the calculated specific capacitances of the nine porous carbon materials prepared in the previous section based on the constant-current charge/discharge curves.The PCs-460 material exhibits a higher performance specific capacitance value than that of the other porous carbon materials, which is up to 422F/g at a current density of 0.5A/g. PCs-460 raw materials contain more light component small molecules, which are more likely to form more micropores under activation conditions, resulting in more storage sites and higher specific capacitance values. The specific capacitance values of oxidized asphalt, hot polymerized asphalt porous charcoal and its soluble component porous charcoal and insoluble component porous charcoal do not change significantly under the three-electrode system, which is mainly due to the fact that oxidized asphalt, hot polymerized asphalt, and its soluble and insoluble components have similar structure of formed pores and the residual substances have the same nature under the activation conditions, and the two-electrode symmetrical capacitor will be used to study the electrochemical under the actual conditions in the follow-up. The electrochemical properties under actual conditions will be investigated using a two-electrode symmetric capacitor. The specific capacitance of Ansteel medium-temperature coal asphalt and its soluble and insoluble components of porous charcoal in the three-electrode system has a large difference, mainly because the asphalt raw material and its soluble and insoluble components of different reactivity with potassium hydroxide under the activation conditions, which leads to the pore structure has a large difference, the existence of the microporous and mesoporous active sites and ion transport channels on the storage and transmission of electrolyte ions also have a large difference. The existence of microporous and mesoporous active sites and ion transport channels has a greater impact on electrolyte ion storage and transport.

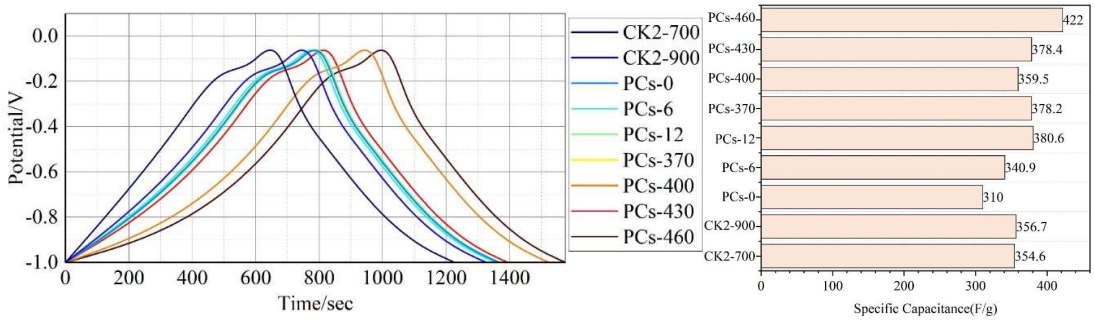

(a) The current density is 0.5a/g's GCD curve (b) Specific capacitance calculated by GCD curves

Figure 2: Constant discharge

The GCD curves and specific heat capacities of PCs-460 at different current densities are shown in Fig. 3, and Fig. 3(a) shows the constant-current charge/discharge curves of PCs-460 at current densities of 0.5 A/g~10 A/g. The charge/discharge curves of PCs-460 at each current density show the symmetric triangular characteristics of a typical bilayer, indicating that the PCs-460 material has a good reversibility of charge/discharge. Fig. 3(b) shows the specific capacitance values corresponding to the constant-current charging and discharging of PCs-460 at current densities from 0.5 A/g to 10 A/g. With the increase of current density. The specific capacitance value of PCs-460 shows a crescent-shaped decreasing trend, and it also has a specific capacitance of more than 290 F/g at a current density of 10 A/g. The constant-current charging and discharging time of PCs-460 material decreases with the increase of current density, which is due to the fact that the ions in the electrolyte do not fully enter into the pores of the porous carbon material under high current density, and the electrode material is not fully in contact with the electrode material for the charging and discharging.

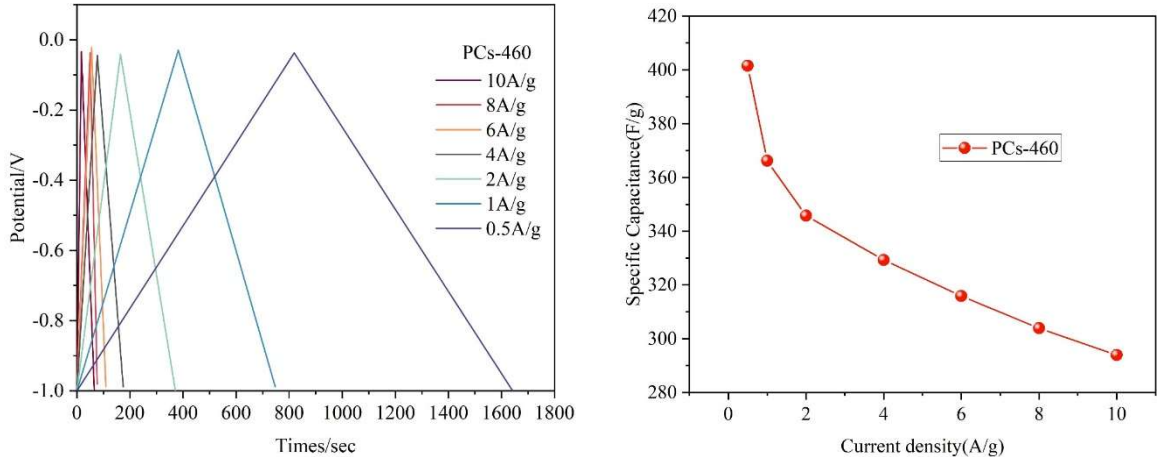

(a) MPC in different current density GCD curves (b) The ratio of the different current density of the MPC

Figure 3: GCD curve and ratio capacitance

(2) Cyclic voltammetry (CV)

The CV curve and specific capacitance at a scan rate of 5 mV/s are shown in Fig. 4. The cyclic voltammetry curves of coal asphalt-based porous carbon materials at a scan rate of 5 mV/s and the specific capacitance values calculated from the absolute area are consistent with the constant-current charging and discharging trends.

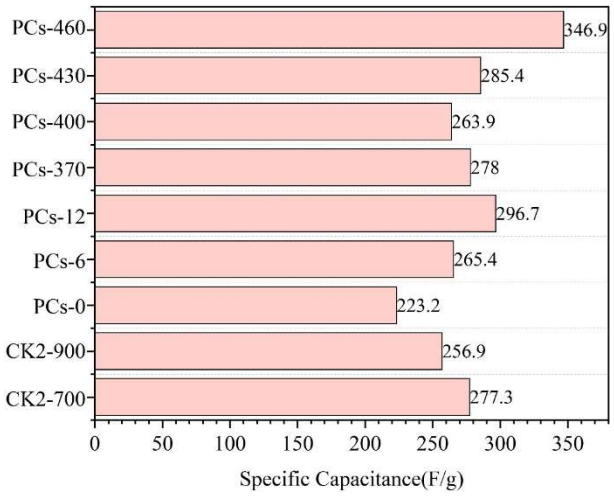

Figure 4: Specific capacitance calculated from CV curves

The CV curves and specific capacitance of PCs-460 at different sweep rates are shown in Fig. 5, and Fig. 5(a) shows the cyclic voltammetry curves of MPC at 5 mV/s~100 mV/s scan rates. All curves show rectangle-like shapes, indicating that the PCs-460 material has good bilayer properties. With the increase of the sweep rate, the absolute

area of the cyclic voltammetry curves of PCs-460 material decreases, and the capacitance performance decreases accordingly. Inevitably, some redox reactions are generated when the voltage window is too low and too high, resulting in a small deformation of the cyclic voltammetry curve. Fig. 5(b) shows the specific capacitance values calculated from the absolute area of cyclic voltammetry curves of MPC at scan rates from 5 mV/s to 100 mV/s. PCs-460 also possesses a specific capacitance of super 210 F/g at a scan rate of 100 mV/s with good reversibility and multiplicity, which has the same trend as the GCD results.

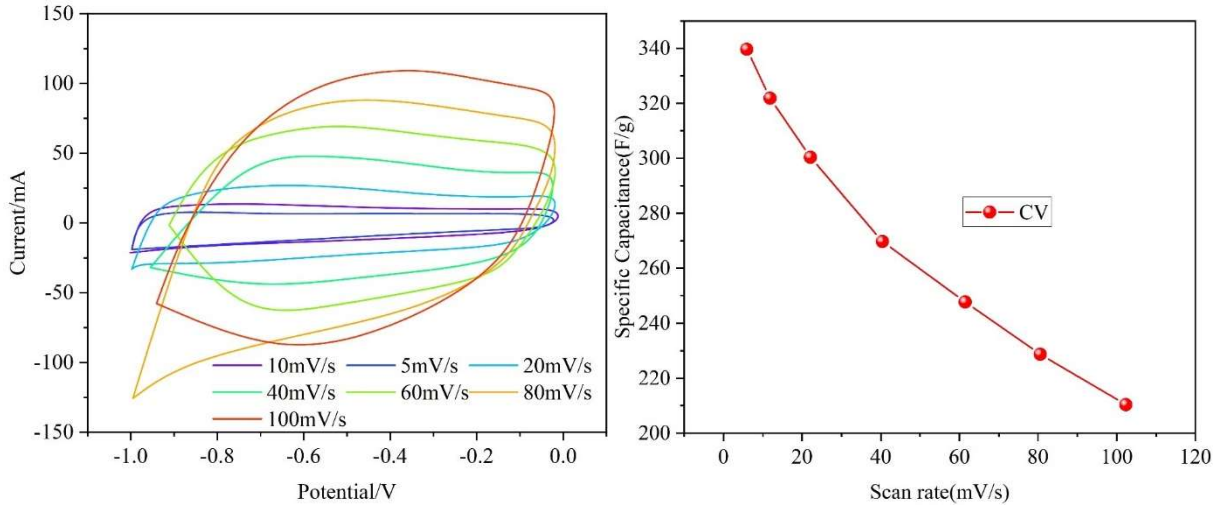

(a) CV curves of MPC at different scanning speeds

(b) Specific capacitance of MPC at different scanning speeds

Figure 5: CV curves and ratio capacitance

(3) AC impedance (EIS)

The results of the analysis of the AC impedance spectra of the nine coal pitch-based porous charcoals are shown in Table 7, which shows the results of the calculation of the ohmic internal resistance Rs, the charge transfer resistance Rct, and the time constant of the nine porous charcoal materials. From the table, it can be seen that the MPC material has the largest ohmic internal resistance Rs = 0.7315 Ω, but its charge transfer resistance is the smallest Rct = 0.1352 Ω. The main reason is that under this activation condition, the generated carbon microcrystalline structure is mostly disordered, which results in a larger internal resistance, but the alkaline charcoal reactivity is the best in this condition, which results in the formation of abundant microporous and mesoporous structures, microporous for the charge storage to provide storage sites, and mesoporous for the storage of charge, and mesoporous for the charge storage. The micropores provide the storage sites for charge storage, and the mesopores provide the fast transmission channel for charge transfer. From the Nyquist chart, we can see that the diameter of the semicircular arc in the high frequency region is the smallest, which indicates that it has the strongest charge transfer ability, and therefore its charge transfer resistance is the smallest.

Table 7: Analysis of ac impedance spectrograph

Sample	Rs (Ω)	Rct (Ω)	τ (s)
PCs-460	0.7315	0.1352	9.8945
PCs-430	0.1808	0.7528	10.6123
PCs-400	0.1736	0.7251	8.0864
PCs-370	0.0964	1.0146	9.6784
PCs-12	0.1289	0.9251	12.6847
PCs-6	0.1932	0.7458	10.0956
PCs-0	5.14×10-6	1.1430	8.0316
CK2-900	0.1345	0.9098	10.5287
CK2-700	0.1930	0.7463	7.8942

III. C. Discussion

The morphology and structure of the porous carbon material were observed using transmission electron microscopy and scanning electron microscopy, and its electrochemical properties were tested by electrochemical workstation, and the following conclusions were obtained.

(1) Under the three-electrode system, PCs-460 exhibits superior capacitance performance, with a specific capacitance of 420 F/g calculated according to the GCD method at a current density of 0.5 A/g, and also has a super 290 F/g specific capacitance value at a current density of 10 A/g.

(2) The specific capacitance value of PCs-460 shows a crescent-shaped decreasing trend, and also has a specific capacitance of more than 290F/g at a current density of 10 A/g. The constant-current charging and discharging time of the PCs-460 material decreases gradually with the increase of current density.

IV. Conclusion

In this study, the effects of asphalt pretreatment on the pore structure and electrochemical behavior of porous carbon were systematically investigated by numerical simulation methods, and the following conclusions were drawn:

Different temperature pretreatments significantly affect the microstructure of asphalt-based porous carbon. With the increase of heat treatment temperature, the carbon layer spacing d002 reaches a maximum value of 0.427 nm at 430 ℃, indicating that the degree of disorder is the largest at this time. The trend of the D-band and G-band integral area ratio AD/AG is consistent with that of d002, and this structural change is mainly originated from the differences in the degree of secondary cross-linking, pyrolysis, and polycondensation reactions at different temperatures. The pretreatment temperature also significantly affected the pore structure characteristics of the porous carbon, and the sample PCs-370 prepared at a heat treatment temperature of 370 °C obtained a maximum specific surface area of 2160 m²/g, with 91% of the microporous volume, which was attributed to the fact that appropriate pretreatment favored the formation of abundant microporous structures.

In terms of electrochemical properties, the sample PCs-460 prepared at a heat treatment temperature of 460 °C showed the best performance, with a specific capacitance of 422 F/g at a current density of 0.5 A/g in the three-electrode system, and maintained a specific capacitance of more than 290 F/g even at a high current density of 10 A/g, which demonstrated excellent multiplicative performance. AC impedance analysis shows that PCs-460 has the smallest charge transfer resistance (Rct=0.1352 Ω) despite its large ohmic internal resistance (Rs=0.7315 Ω), which is attributed to its abundant microporous and mesoporous structure that provides both sufficient active sites for charge storage and a smooth channel for ion transfer.

In summary, the microstructure and pore size distribution of asphalt-based porous carbon can be effectively regulated by a reasonable pretreatment method, which in turn optimizes its electrochemical performance. The results of this study provide theoretical guidance and experimental basis for the design and preparation of high-performance asphalt-based porous carbon materials.

References

[1] Guo, M., Liang, M., Jiao, Y., Zhao, W., Duan, Y., & Liu, H. (2020). A review of phase change materials in asphalt binder and asphalt mixture. Construction and Building Materials, 258, 119565.

[2] Jain, S., & Singh, B. (2021). Cold mix asphalt: An overview. Journal of cleaner production, 280, 124378.

[3] Cheraghian, G., Falchetto, A. C., You, Z., Chen, S., Kim, Y. S., Westerhoff, J., ... & Wistuba, M. P. (2020). Warm mix asphalt technology: An up to date review. Journal of Cleaner Production, 268, 122128.

[4] Hou, X., Lv, S., Chen, Z., & Xiao, F. (2018). Applications of Fourier transform infrared spectroscopy technologies on asphalt materials. Measurement, 121, 304-316.

[5] Du, S. X., Kong, L. Y., Liu, L., Cao, Z. Y., Wu, X., Sun, B., ... & Li, Y. F. (2024). A review of petroleum asphalt-based carbon materials in electrochemical energy storage. New Carbon Materials, 39(6), 1088-1107.

[6] Wang, Q., Fagbohun, E. O., Zhu, H., Hussain, A., Wang, F., & Cui, Y. (2023). One-step synthesis of magnetic asphalt-based activated carbon with high specific surface area and adsorption performance for methylene blue. Separation and Purification Technology, 321, 124205.

[7] Liang, W., Xiao, H., Lv, D., Xiao, J., & Li, Z. (2018). Novel asphalt-based carbon adsorbents with super-high adsorption capacity and excellent selectivity for separation for light hydrocarbons. Separation and Purification Technology, 190, 60-67.

[8] Gorbunova, O. V., Baklanova, O. N., Gulyaeva, T. I., Arbuzov, A. B., Trenikhin, M. V., & Lavrenov, A. V. (2022). Effect of thermal pretreatment on porous structure of asphalt-based carbon. Journal of Materials Science, 57(14), 7239-7249.

[9] Hasan, M. R. M., Chew, J. W., Jamshidi, A., Yang, X., & Hamzah, M. O. (2019). Review of sustainability, pretreatment, and engineering considerations of asphalt modifiers from the industrial solid wastes. Journal of Traffic and Transportation Engineering (English Edition), 6(3), 209-244.

[10] Behravan, A., Lowry, M., Ashraf-Khorasani, M., Tran, T. Q., Feng, X., & Brand, A. S. (2023). Effect of pretreatment on reclaimed asphalt pavement aggregates for minimizing the impact of leachate on cement hydration. Cement and Concrete Research, 173, 107305.

[11] Sun, J., Huang, W., Wang, X., Hu, J., Wang, Y., Zhang, Z., & Luo, S. (2024). Feasibility of pretreated steel slag for asphalt pavement application and risk assessment of hazardous substance leaching. Chemical Engineering Journal, 498, 155497.

[12] Xiao, R., Polaczyk, P., & Huang, B. (2024). Mitigating stripping in asphalt mixtures: pretreatment of aggregate by thermoplastic polyethylene powder coating. Transportation Research Record, 2678(4), 776-787.

[13] Zhang, J., Chen, M., Wu, S., Zhao, Y., Fan, Y., & Chen, D. (2025). Aging behavior and microscopic characteristics of modified asphalt using different pretreated crumb rubber. Construction and Building Materials, 462, 139955.
[14] Xiong, H., & Zheng, H. (2025). Study on the effect of asphalt pretreatment on the structural and electrochemical properties of porous carbon based on finite element analysis. J. COMBIN. MATH. COMBIN. COMPUT, 127, 6849-6866.
[15] Gorbunova, O. V., Baklanova, O. N., Gulyaeva, T. I., & Lavrenov, A. V. (2021). EFFECT OF ALKALINE ACTIVATION CONDITIONS ON POROUS STRUCTURE OF PETROLEUM ASPHALT-BASED CARBON. In Physicochemical problems of adsorption, structure, and surface chemistry of nanoporous materials (pp. 80-81).
[16] Wang, Q., Zhang, Y., Hussain, A., Guo, Z., Wang, L., & Cui, Y. (2025). Asphalt-derived hierarchical porous carbon as an efficient adsorbent for benzene. Separation and Purification Technology, 353, 128467.
[17] Jalilov, A. S., Ruan, G., Hwang, C. C., Schipper, D. E., Tour, J. J., Li, Y., ... & Tour, J. M. (2015). Asphalt-derived high surface area activated porous carbons for carbon dioxide capture. ACS applied materials & interfaces, 7(2), 1376-1382.
[18] Tingsen Zhang,Zhiyong Deng,Weiwei Wu,Fei Liu & Yingying Jian. (2025). A special two-working-electrode system: a summary of recent development in fabrication and application of interdigitated array electrodes .Nanotechnology,36(13),132001-132001.
[19] Li Yao,Long Jin,Liang Yun & Hu Jian. (2023). Lithium dendrites puncturing separator induced galvanostatic charge/discharge test problem in Li-symmetric cells. Ionics,29(11),4933-4938.
[20] Jian Yu,Xingyu Li,Qi Zhang,Wenliang Li,Ming Zhou,Yunhuai Zhang & Peng Xiao. (2025). Amorphous/crystalline hetero-phase Ni-doped Co/CoP: Cyclic voltammetry synthesis and energy-efficient hydrazine-assisted water splitting via N-N breakage. Applied Catalysis B: Environment and Energy,373,125374-125374.
[21] Selvaraj Chinnathambi,Mohammad Saghafi,Suryasnata Tripathy,Frans P. Widdershoven & Serge G. Lemay. (2025). High-frequency electrochemical impedance measurements of self-assembled monolayer formation using CMOS-based nanocapacitor arrays. Sensors and Actuators Reports,9,100293-100293.
[22] Li Cui,Yimin Wang,Zhen Yuan,Xiaoli Zhang,Yuewen Chen,Xiya Zhang... & Hai Liu. (2025). Benchmarking catalytic activity and cyclic stability of glycerol oxidation to dihydroxyacetone over bio-templated porous ZSM-5 platform composite with Au/CuO. International Journal of Hydrogen Energy,119,1-12.